Journal of Virological Methods 262 (2018) 12–19

Contents lists available at ScienceDirect

Journal of Virological Methods

journal homepage: www.elsevier.com/locate/jviromet

A qPCR assay for measuring the post-integrational DNA repair in HIV-1 replication

Andrey N. Anisenko[a,*], Ekaterina S. Knyazhanskaya[b,c], Maria G. Isaguliants[d,e], Marina B. Gottikh[b,c]

[a] Faculty of Bioengineering and Bioinformatics, Lomonosov Moscow State University, Moscow, Russia
[b] Chemistry Department, Lomonosov Moscow State University, Moscow, Russia
[c] Belozersky Institute of Physico-Chemical Biology, Lomonosov Moscow State University, Moscow, Russia
[d] Ivanovsky Institute of Virology, Moscow, Russia
[e] Department of Microbiology, Tumor and Cell Biology, Karolinska Institutet Stockholm, Sweden

ARTICLE INFO

Keywords:
HIV
Integration
DNA repair
qPCR
DNA-PK
DNA-PKcs

ABSTRACT

The post-integrational gap repair is a critical and poorly studied stage of the lentiviral life cycle. It might be performed by various cellular DNA repair pathways but the exact mechanism of the repair process has not yet been described. One of the reasons for that is the lack of a functional quantitative assay that could precisely measure the amount of integrated viral DNA that has completed the post-integrational gap repair stage. Here, we present an approach that is based on a widely used Alu-specific PCR for the estimation of integrated viral DNA but includes several steps that allow discrimination between integrated-repaired and integrated-unrepaired viral DNA forms. We used the approach for the estimation of the kinetics of gap repair in a viral vector system and showed that the gap repair process starts at 17 h post infection and lasts 10 more hours. We also showed that the addition of Nu7441 – a small molecule inhibitor of DNA-breaks sensor kinase in the non-homologous end joining DNA repair pathway – specifically inhibits the gap repair process while having no influence on the integration itself.

1. Introduction

The early stages of HIV-1 (Order *Ortervirales*, Family *Retroviridae*, Subfamily *Orthoretroviridae*, species *Human immunodeficiency virus type 1*) infection involve the entry of the viral core into the cell cytoplasm, reverse transcription resulting in the formation of a linear double stranded DNA copy of the viral genomic RNA, and integration of the viral DNA into the host cell DNA (Cimarelli and Darlix, 2014; Freed and Mouland, 2006; Lewinski and Bushman, 2005; Lesbats et al., 2016). Formation of an integrated viral genome, which is referred to as the provirus, is obligatory for efficient viral replication. The integration is catalyzed by the viral enzyme integrase that inserts viral DNA into the host genome in two distinct reactions named 3'-processing and strand transfer (Engelman et al., 1991; Delelis et al., 2008). During 3'-processing, integrase cleaves GT dinucleotides from both 3'-ends of viral DNA liberating 3'-hydroxyl groups. Then, within the strand transfer, integrase utilizes these 3′-hydroxyls as nucleophiles to cut the host DNA, simultaneously inserting 3′-ends of the viral DNA into the opposing strands of host DNA. The sites of the nucleophilic attack are located five nucleotides apart from each other (Lewinski and Bushman, 2005; Lesbats et al., 2016; Engelman et al., 1991; Delelis et al., 2008). The resulting product is generally referred to as integration intermediate and represents a viral DNA flanked by five nucleotide gaps and containing two unpaired nucleotides at each 5'-overhanging end (Fig. 1A). The repair of these genomic discontinuities is considered to be carried out by the cellular DNA repair enzymes (Lesbats et al., 2016). However, it should be noted that the precise repair mechanism as well as enzymes that carry out this process are not exactly ascertained.

Post-integrational gap repair enzymes might be identified by using biochemical and/or genomic approaches. A number of genome scale siRNA screens has been performed, which allowed determining more than 1000 different host factors associated with HIV replication, including enzymes participating in different DNA repair systems (Brass et al., 2008; König et al., 2008; Zhou et al., 2008). Unfortunately, there is little overlap between the sets of host proteins identified in each screen. Each of the screens has identified at least one DNA repair protein; however, summarizing the results of all the screens it is impossible to conclusively point at a DNA repair pathway that is responsible for the

* Corresponding author.
E-mail address: a_anisenko@mail.ru (A.N. Anisenko).

https://doi.org/10.1016/j.jviromet.2018.09.004
Received 5 June 2018; Received in revised form 11 September 2018; Accepted 12 September 2018
Available online 13 September 2018

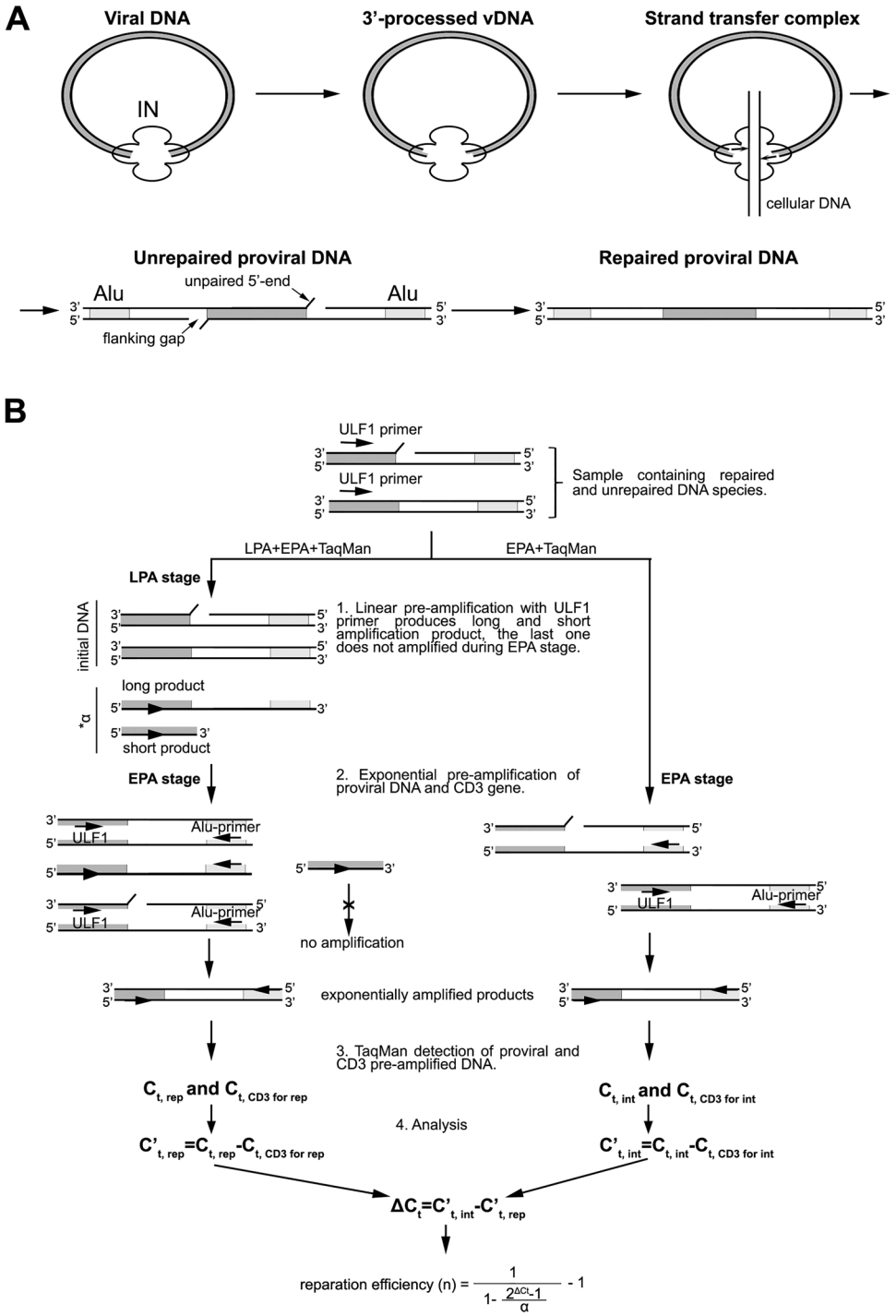

Fig. 1. Quantitative measurement of the post-integrational gap repair efficiency. A – Unrepaired (I–U) and repaired (I–R) proviral DNA structure; B – general scheme of the PCR-based assays used to measure the gap repair efficiency: α – the number of cycles in linear pre-amplification stage, LPA – linear pre-amplification, EPA – exponential pre-amplification.

integration intermediate repair. An siRNA screen specifically targeting DNA repair genes identified several proteins throughout the short patch base excision repair (BER) pathway that appear to be important for HIV integration (Espeseth et al., 2011; Yoder et al., 2011). However, the mechanism of the BER proteins' participation in HIV integration remains obscure. It might involve, for example, the influence of BER events in the host genome on HIV integration site selection (Bennett et al., 2014).

At the same time, many biochemical and virological studies demonstrate that DNA double strand break (DSB) repair enzymes are necessary for efficient retroviral infection, especially for the post-integration repair and/or circularization of the viral DNA (Daniel et al., 2001; Li et al., 2001; Sakurai et al., 2009; Smith et al., 2008; Yoder and Bushman, 2000). The role of enzymes from nonhomologous end-joining (NHEJ) pathway is particularly widely studied (Cooper et al., 2013; Daniel et al., 1999; Li et al., 2001; Smith et al., 2008), but nevertheless all of the efforts to date have not definitively clarified the mechanism of repair of the gapped-integration intermediate. One of the reasons for this may be the lack of methods for a direct measurement of HIV-1 post-integrational gap repair efficiency in the cell.

Here we present a novel assay for a quantitative estimation of HIV-1 post-integrational gap repair, which is based on a previously published variant of Alu-specific PCR (Vandergeeten et al., 2014). Alu-repeats are repetitive DNA sequences widely dispersed throughout the human genome. Alu-specific PCR is a rapid and ultrasensitive method for quantitative measurement of the integrated HIV-1 DNA. It consists of two steps: 1) an amplification of integrated DNA together with a fragment of genomic DNA using one primer annealing to the HIV-1 LTR-sequence and another one annealing to Alu-repeat; 2) a quantitative measurement of integrated DNA using a different set of primers complementary to the LTR region of viral DNA. By adding a modification to this published assay, we succeeded in the determination of the kinetics of DNA gap repair in a cellular model of HIV infection. In addition, we analyzed the effect of inhibition of one of the components of NHEJ system, the catalytic subunit of DNA-dependent protein kinase, DNA-PKcs, on post-integrational DNA gap repair and demonstrated that DNA-PKcs is indeed a positive factor of this process.

2. Materials and methods

2.1. Cell culture, viral assembly, infection and analysis

HEK293 T cells were cultured in DMEM medium supplemented with 10% FBS and penicillin/streptomycin solution (all obtained from Invitrogen). J-Lat cells were cultured in RPMI medium supplemented with 10% FBS and penicillin/streptomycin solution. Viral vectors were assembled as described in (Mazurov et al., 2010). pCMVΔ8.2R viral packaging plasmid and pCMV VSV-G plasmid were obtained from Addgene. pUCHR_inLuc HIV genomic plasmid was a kind gift of Dr. D. Mazurov. Viral stocks were concentrated by centrifugation at 30,000*g* and resuspended in 1xPBS. p24 was analyzed using the HIV-1 p24-antigen IFA kit (Vector Best). Cells were infected by adding the virus to the cell media at final concentration of 10 pg of p24 per 10^5 cells and at indicated h.p.i. timepoints, cells were harvested and counted and luciferase activity in cell lysates was assayed using the Luciferase assay system kit (Promega). For the DNA-PKcs inhibition assay, Nu7441 (Seleckchem) or DMSO were added to cell medium simultaneously with viral transduction. Stock solution of Nu7441 was prepared in 100% DMSO according to the manufacturer's instructions.

2.2. Total DNA extraction

$1*10^6$ HEK293 T cells were resuspended in 200 µL of lysis buffer (10 mM Tris-HCl, pH 8.0, 50 mM KCl, 2 mg/mL proteinase K; Thermo Scientific) and digested for 12 h at 55 °C in a heating shaker. Proteinase K was inactivated by heating at 95 °C for 10 min and extracted three times with phenol:chlorophorm:isoamyl alcohol in the ratio of 25:24:1.

2.3. Total and integrated viral DNA quantification

The amount of the total and integrated viral DNA was measured as described in (Vandergeeten et al., 2014). Primer sequences and descriptions are shown in Table 1.

To quantitatively estimate the gap repair efficiency, 200–400 ng of total DNA obtained from infected cells was divided between two PCR tubes. In all PCR reactions, primers specific for the human CD3 gene (primers HCD3OUT5′ and HCD3OUT3′) were used to quantify the exact number of cells present in the reaction tube (Table 1). The pre-amplification of the total HIV DNA and the CD3 gene was carried out in a 50-µL reaction mixture comprising 1 × DreamTaq polymerase buffer (Thermo), 3 mM $MgCl_2$, 300 µM deoxynucleoside triphosphates (Thermo), 300 nM each of the 4 primers (primers ULF1, UR1, HCD3OUT5′, and HCD3OUT3′), and 2.5 U DreamTaq polymerase (Thermo). The first-round PCR cycle conditions are as follows: a denaturation step of 8 min at 95 °C and 12 cycles of amplification (95 °C for 1 min, 55 °C for 40 s, 72 °C for 1 min), followed by a final elongation step at 72 °C for 15 min.

Integrated HIV DNA was amplified in the same mixture as that used for the total HIV DNA quantification, with the exception that the reverse primer (UR1) was replaced by the Alu1 and Alu2 primers (300 nM each) and the concentration of ULF1 was reduced (150 nM). Given the high number of Alu elements in the human genome, abundant amplifications of inter-Alu sequences occurred simultaneously with the amplification of Alu-LTR sequences. To remain within the exponential phase, only 12 cycles of amplification were performed. The PCR cycle conditions were as follows: a denaturation step of 8 min at 95 °C and 12 cycles of amplification (95 °C for 1 min, 55 °C for 1 min, 72 °C for 10 min), followed by an elongation step of 15 min at 72 °C.

The second round of PCR was carried out in real time on a Biorad CFX96 amplifier (Biorad). All reactions (for total HIV DNA, integrated HIV DNA, and CD3) were performed in a final volume of 20 µL containing 3 µL of a 1/10 dilution of the PCR products obtained during the first round. Appropriate sets of primers (1.250 nM Lambda T and UR2 for total and integrated HIV DNA, Lambda T and ULTRR2 for 2-LTR circles, and HCD3IN5′ and HCD3IN5′ for the CD3 gene) were added to the Rotor-Gene probe master mixture. The UHIV TaqMan probe (200 nM) was added to the total and integrated HIV DNA reaction mixtures, whereas the same concentration of the U2LTR TaqMan probe was used for the 2-LTR reaction. For CD3 quantification, 200 nM of the CD3 TaqMan probe was used. The same amplification steps are used for all reactions: a denaturation step (95 °C for 4 min), followed by 40 cycles of amplification (95 °C for 3 s, 60 °C for 10 s).

The TaqMan PCR was carried out on a Biorad CFX96 amplifier (Biorad) with the Taq DNA-polymerase (Thermo) following the manufacturer's instructions. All reactions were performed in a final volume of 20 µL containing 5 µL of a 1/5 dilution of the PCR products obtained during the first round. The set of primers (250 nM Lambda T and UR2 for the total and integrated HIV DNA, and HCD3IN5′ and HCD3IN5′ for the CD3 gene) was added to the master mix. The UHIV TaqMan probe (200 nM) was added to total and integrated reaction mixtures. For CD3 quantification, 200 nM of the CD3 TaqMan probe is used. The same amplification steps were used for all reactions: a denaturation step (95 °C for 4 min), followed by 40 cycles of amplification (95 °C for 10 s, 60 °C for 20 s).

2.4. Gap repair efficiency estimation

1 To quantitatively estimate the gap repair efficiency, 200–400 ng of total DNA obtained from infected cells was divided between two PCR tubes.
2 Tube 1 (signed as "rep" in which the linear preamplified integrated DNA was measured) included 150 nM ULF1 primer, 1X DreamTaq buffer, 1.25 U of DreamTaq polymerase, dNTP mix (0.4 mM of each) and 1 mM $MgCl_2$. Total volume = 20 µL.
3 The linear pre-amplification (LPA) cycling conditions:
Step 1: 95 °C 8 min
Step 2: 95 °C 1 min
Step 3: 55 °C 1 min
Step 4: 72 °C 10 min
Number of cycles (steps 2–4): 24
Step 5: 72 °C 15 min
4 After finishing the LPA stage 5 µL of 1X DreamTaq buffer with 300 nM of each Alu1, Alu2, HCD3OUT3', and HCD3OUT5' primers, dNTP mix (0.4 mM of each) and 1 mM $MgCl_2$ were added to tube 1.
5 The exponential pre-amplification (EPA) cycling conditions:
Step 1: 95 °C 3 min
Step 2: 95 °C 1 min
Step 3: 55 °C 1 min
Step 4: 72 °C 10 min
Number of cycles (steps 2–4) 12
Step 5: 72 °C 15 min
Note: To remain within the exponential amplification phase, the

Table 1
Oligonucleotides used for quantitative estimation of total and integrated HIV-1 DNA and post-integrational gap repair efficiency.

Name	Sequence (5'-3')	Target (Position in HXB2)
ULF1	ATGCCACGTAAGCGAAACTCTGGGTCTCTCTGGTTAGAC	U3-R junction of viral LTR (452–471)
Alu1	TCCCAGCTACTGGGGAGGCTGAGG	Human Alu-sequence (NA)
Alu2	GCCTCCCAAAGTGCTGGGATTACAG	Human Alu-sequence (NA)
UR1	CCATCTCTCTCCTTCTAGC	Viral LTR (U5) - Gag (775–793)
LambdaT	ATGCCACGTAAGCGAAACT	18bp 5'-sequence of ULF1 primer – LTR (NA)
UR2	CTGAGGGATCTCTAGTTACC	U5 region of viral LTR (583–602)
HCD3OUT3'	ACTGACATGGAACAGGGGAAG	Human CD3 gene (NA)
HCD3OUT5'	CCAGCTCTGAAGTAGGGAACATAT	Human CD3 gene (NA)
HCD3IN5'	GGCTATCATTCTTCTTCAAGGT	Human CD3 gene (NA)
HCD3IN3'	CCTCTCTTCAGCCATTTAAGTA	Human CD3 gene (NA)
UHIV_TaqMan	FAM-GCACTCAAGGCAAGCTTTATTGAGG-BHQ-1	R region of viral LTR (522–546)
CD3_TaqMan	FAM-AGCAGAGAACAGTTAAGAGCCTCCAT-BHQ-1	Human CD3 gene (NA)

number of cycles on the EPA stage should not exceed 12.

6 Into tube 2 (signed as "int" in which the integrated viral DNA was measured) 150 nM ULF1 should be added together with 300 nM of each Alu1, Alu2, HCD3OUT3', and HCD3OUT5' primers, 1X DreamTaq buffer, 1.25 U of DreamTaq polymerase, dNTP mix (0.4 mM of each) and 1 mM $MgCl_2$. Total volume = 25 µL. The EPA procedure was performed as described in 5.

7 The TaqMan PCR was carried out on a Biorad CFX96 instrument (Biorad) with the Taq DNA-polymerase (Thermo) following the manufacturer's instructions. All reactions (for "repaired" HIV DNA, integrated HIV DNA, and CD3) were performed in a final volume of 20 µL containing 5 µL of a 1/5 dilution of the PCR products obtained in EPA stage. The appropriate sets of primers (250 nM Lambda T and UR2 for "repaired" and integrated HIV DNA, and HCD3IN5′ and HCD3IN5′ for the CD3 gene) were added to the master mix. The UHIV TaqMan probe (200 nM) was added to tube 1 ("rep") and tube 2 ("int") reaction mixtures. For CD3 quantification, 200 nM of the CD3 TaqMan probe was used. The same amplification steps were used for all reactions: a denaturation step (95 °C for 4 min), followed by 40 cycles of amplification (95 °C for 10 s, 60 °C for 20 s).

8 For each sample four C_t values were obtained: $C_{t,\ rep}$ (integrated viral DNA with linear pre-amplification) $C_{t,\ CD3\ for\ rep}$, $C_{t,\ int}$ (integrated viral DNA without linear pre-amplification), and $C_{t,\ CD3\ for\ int}$. Then, $C_{t,\ rep}$ and $C_{t,\ int}$ were normalized to the amount of CD3 gene in the same sample.

$C'_{t,\ rep} = C_{t,\ rep} - C_{t,\ CD3\ for\ rep}$ and $C'_{t,\ int} = C_{t,\ int} - C_{t,\ CD3\ for\ int}$.

$\Delta C_t = C'_{t,\ int} - C'_{t,\ rep}$

- Using the formula (6), the repair efficiency was calculated from ΔC_t value.

  Of note, these primers are suitable for amplification of HIV sequences from the 6 major circulating subtypes (A, B, C, D, CRF01_A/E [A/E], and CRF01_A/G [A/G], which account for 85% of global HIV-1 variants) (Vandergeeten et al., 2014).

2.5. Data analysis

The reported values are the average of three independent measurements expressed as mean ± standard deviation.

3. Results

3.1. General method description

The integration of the retroviral DNA in the cellular genome is catalyzed by the viral enzyme integrase (Lewinski and Bushman, 2005; Lesbats et al., 2016; Engelman et al., 1991; Delelis et al., 2008). Its activity results in the formation of an integration intermediate (Fig. 1A, left panel) that has to be repaired by cellular DNA repair machinery for the viral genes to be expressed (Skalka and Katz, 2005). A widely used approach to quantitatively measure the amount of integrated DNA involves preamplification of the viral DNA using primer pairs where one anneals to a certain repeated genomic locus (usually Alu repeat (Vandergeeten et al., 2014)) and the other anneals to a region within proviral DNA. Thus, only the integrated viral DNA is exponentially amplified and measured as opposed to reverse transcribed cDNA and circular episomal 2-LTR and 1-LTR forms, due to the absence of Alu repeats. Despite its high efficiency in quantitative determination of the amount of integrated DNA, this approach cannot precisely distinguish between integrated-repaired (I–R) and integrated-unrepaired (I–U) forms of proviral DNA. The persistence of the gapped integration intermediates can maximally yield in theory a twofold (1-cycle) decrease in the amplification assay (Jeanson et al., 2002). To adapt Alu-specific PCR for the measurement of an I–U form we added a linear pre-amplification stage to the protocol. The DNA sample containing integrated viral DNA is firstly subjected to a linear PCR with an ULF1 primer (Table 1), that anneals to the U3-R junction of viral LTR (linear pre-amplification, LPA). The use of an ULF1 primer in case of I–R form allows the synthesis of a long product, which potentially contains an Alu-sequence; whereas in the case of I–U form polymerase reaction stops at the gap, and only the short product which does not contain an Alu-sequence is synthesized (Fig. 1B).

The second stage is a one tube exponential pre-amplification (EPA) of 1) the integrated form of viral DNA using Alu1, Alu2, and ULF1 primers and 2) CD3 gene as a reference gene using HCD3OUT3' and HCD3OUT5' primers (Table 1). Importantly, on this stage, amplification of the integrated form of viral DNA occurs only from initial DNA (both I–R and I–U) and from the long product that is produced on the LPA stage. The short product cannot be amplified on the second stage due to the lack of Alu-sequence (Fig. 1B). On the third step, a final quantitative measurement of I–R viral DNA and CD3 gene is performed using specific TaqMan probes (Vandergeeten et al., 2014). For a correct estimation of the fraction of I–R form in the total integrated viral DNA, the same amount of initial DNA passes through the second (EPA) and the third stage to quantitatively measure total integrated DNA (I–R + I–U) in the same sample.

For both procedures (LPA + EPA + TaqMan PCR and EPA + TaqMan PCR) the Ct values are obtained for each sample. The difference between normalized Ct obtained by the two procedures shows the level of gap-repair.

3.2. Theoretical calculations

Assuming that a given sample contains x integrated HIV genomes and n is the proportion of I–R molecules, therefore the sample contains nx I–R HIV genomes and $(1-n)x$ I–U HIV genomes. On the first step, one performs LPA with the ULF1 primer only. Performing α cycles of LPA leads to the formation of αnx single-stranded long products, which can then be amplified on the EPA stage. In the beginning of EPA the tube

contains *nx* molecules of initial I–R DNA, *αnx* single-stranded long products, and *(1-n)x* molecules of I–U DNA. After the addition of Alu-specific primers to the reaction mixture, *nx* I–R DNA molecules are exponentially amplified in all the cycles starting in the first one, while the *(1-n)x* I–U DNA and *αnx* long LPA products are also exponentially amplified, but the first cycle is used for dsDNA generation based on ssDNA template (long LPA products) or dsDNA template containing a gap in one strand (I–U DNA) (Fig. 1B). Therefore, the amount of DNA that can be detected during TaqMan PCR followed LPA and EPA equals to:

$$DNA_{rep} = 2^{\varphi} \bullet n \bullet x + \frac{2^{\varphi}}{2} \bullet (1-n) \bullet x + \frac{2^{\varphi}}{2} \bullet \alpha \bullet n \bullet x, \quad (1)$$

where α is the number of cycles on the LPA stage, φ – number of cycles in EPA stage, n – portion of I–R DNA.

The tube in which total integrated DNA is measured (EPA + TaqMan PCR) contains

$$DNA_{int} = 2^{\varphi} \bullet n \bullet x + \frac{2^{\varphi}}{2} \bullet (1-n) \bullet x \quad (2)$$

Using the assumption, that $C_t = C_1 - log_2 DNA$, where C_1 is a threshold cycle for a sample containing 1 molecule, ΔC_t equals to:

$$\Delta C_t = C_{t,int} - C_{t,rep} = C_1 - log_2 DNA_{int} - C_1 + log_2 DNA_{rep} \quad (3)$$

$$\Delta C_t = log_2 \frac{DNA_{rep}}{DNA_{int}} \quad (4)$$

After all algebraic transformations (see Supplementary file),

$$\Delta C_t = log_2 \left(\frac{\alpha \bullet n}{n+1} + 1 \right) \quad (5)$$

This calculation demonstrates that ΔC_t only depends on the proportion of the repaired provirus (n) and the number of cycles on the LPA stage (α), and does not depend on the initial amount of the integrated DNA or the number of cycles on the EPA stage. The Fig. 2A demonstrates the dependence of ΔC_t on the number of cycles on the LPA stage. The maximal ΔC_t will equal 3.7 when n = 1 and α = 24 (Fig. 2B). The optimal cycle number during LPA was shown to be within the 14–24 range, with a maximum ΔC_t for a 14-cycle amplification equal to 3.0 and a maximum ΔC_t for a 24-cycle amplification equal to 3.7. Lowering the cycle number will significantly decrease the sensitivity of the method whereas an increase in the cycle number will prolong the sample preparation time and might cause stronger background signal.

An inverse function to calculate viral DNA repair efficiency based on experimental ΔC_t values (detailed calculations are described in Supplementary file) is as follows:

$$n = \frac{1}{1 - \frac{2^{\Delta C_t} - 1}{\alpha}} - 1 \quad (6)$$

This equation explains how to transform experimental data (difference between C_t value for integrated DNA obtained during EPA + TaqMan procedure and C_t value for repaired DNA obtained during LPA + EPA + TaqMan procedure) into gap-repair efficiency.

3.3. Method validation

To validate the method for gap repair efficiency estimation, we used a sample with known proviral DNA repair efficiency. The J-Lat cell line is derived from Jurkat cells and contains a stably integrated latent HIV-1 derived proviral genome (Fernandez and Zeichner, 2010). The latent infection status implies that all the proviruses are repaired in these cells (n in Eq. (6) equals 1). Here and below, we used 24 cycles of LPA. We determined the ΔC_t for J-Lat cell line as 3.66 ± 0.1, which corresponds to a 95 ± 14% repair efficiency (mean ± SD, 6 repeats). The calculated value of the repair efficiency is consistent with the theoretical value of the repair level of proviral DNA in this cell type (100%).

3.4. Determination of kinetics of post-integrational gap repair

The above validated method was further applied to determine the kinetics of gap repair in a cellular model of HIV infection. We used a single round VSV-G pseudotyped firefly luciferase expressing vector based on HIV-1 (Mazurov et al., 2010) and HEK 293 T cells. First, using the previously described method (Vandergeeten et al., 2014), we identified the absence of detectable changes in the amount of total DNA 12 h.p.i. and integrated DNA 17 h.p.i. (Fig. 3A–B), therefore, the reverse transcription and integration of the viral DNA in our conditions are completed at these time points. Using the gap repair estimation method presented here, we measured the kinetics of post-integrational gap repair (Fig. 3C). This process does not start until the 17 h.p.i. time point and needs about 10 h to achieve 100% repair efficiency in HEK 293T cells (Fig. 3E). This finding is corroborated by the fact that the luciferase activity in cell lysates, that indicates the production of viral proteins, cannot be detected either until the initiation of gap repair (Fig. 3D).

3.5. DNA-PKcs kinase activity is essential for HIV-induced gap repair

We then investigated the effect of a known repair factor on the amount of I–R viral DNA form. The detailed mechanism of the post-integrational gap repair has not yet been described, but the positive effect of DNA-dependent protein kinase (DNA-PK) on lentiviral infectivity and post-infection cell survival has been mentioned (Baekelandt et al., 2000; Skalka and Katz, 2005). DNA-PK acts as a DSB sensor and an effector kinase within the NHEJ pathway (Ariumi et al., 2005; Knyazhanskaya et al., 2016; Ma et al., 2005). DNA-PK consists of 3 different subunits: Ku70, Ku80, and the catalytic subunit – DNA-PKcs. In the present study we investigated the effect of DNA-PKcs inhibition by a specific inhibitor Nu7441 (Leahy et al., 2004) on post-integrational gap repair efficiency. For this purpose, HEK 293T cells treated with Nu7441 and control DMSO-treated cells were transduced by the VSV-G pseudotyped single round HIV-based vector carrying a firefly luciferase transgene (Mazurov et al., 2010). The post-integrational gap repair efficiency was measured 27 h post infection, which is the time point

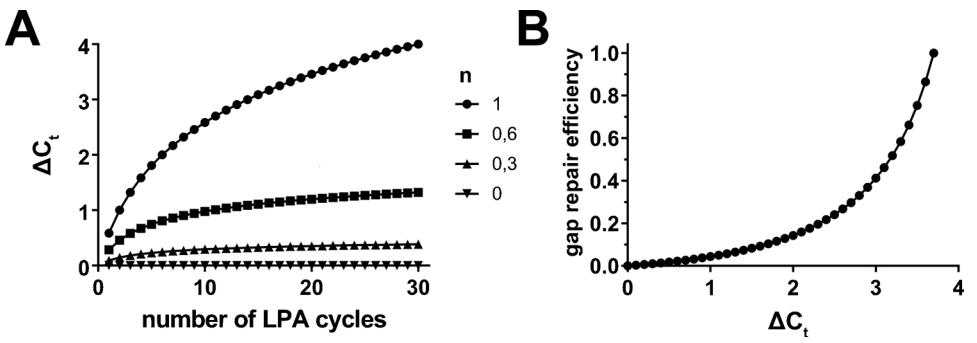

Fig. 2. Theoretical calculations for evaluation of the post-integrational gap repair efficiency. A – Dependence of ΔC_t on α (the number of cycles in LPA stage) for samples with different proportion of I–R DNA (n – gap repair efficiency); B – dependence of the post-integrational gap repair efficiency on ΔC_t in case of 24 cycles in LPA stage.

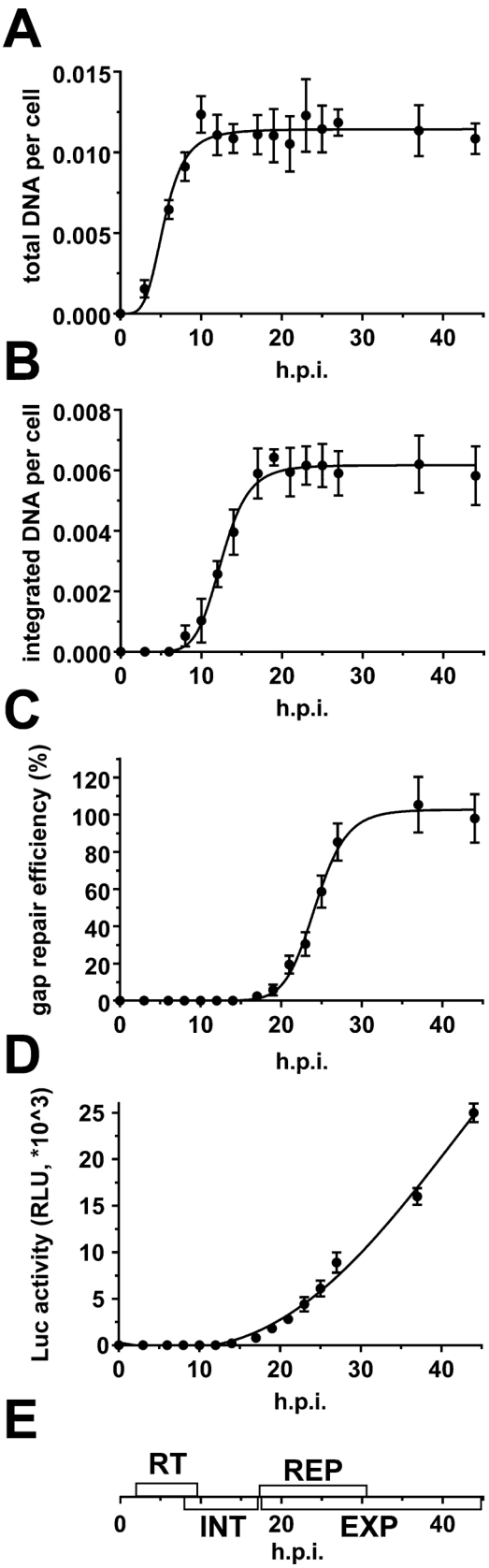

Fig. 3. Analysis of different forms of viral DNA in HEK 293T cells infected by VSV-G pseudotyped single round HIV-based vector. A–B – Kinetics of accumulation of total (A) and integrated (B) viral DNA in cells determined by qPCR-method (Vandergeeten et al., 2014), C – kinetics of post-integrational gap repair determined by the modified variant of Alu-specific PCR, D – kinetics of luciferase production in infected cells, E –HIV-1 life cycle events on the time scale (h.p.i. - hours post infection). RT- reverse transcription, INT – integration, REP – post-integrational gap repair, EXP – transgene expression.

where the post-integrational gap repair is completed by approximately 95% in our hands (Fig. 3C). We found that the addition of Nu7441 decreases post-integrational gap repair efficiency 4.3-times, from 95 + / − 7% to 23 + / − 4% (Fig. 4C). The similar effect was observed when we analyzed the Nu7441 influence on the level of luciferase activity (Fig. 4D, 100 + / − 15% in control vs 43 + / − 11% in Nu7441 treated cells). At the same time, the levels of total and integrated DNA in both control and Nu7441-treated cells were similar (Fig. 4A and B). Thus, DNA-PKcs is indeed involved in the post-integrational gap repair and does not affect either reverse transcription or integration.

4. Discussion

Despite decades of extensive research into HIV-1 and retroviral replication in general, the post-integration gap repair remains poorly studied. It has been generally considered that the cellular DNA repair machinery performs the filling of the gaps, the processing of the unpaired dinucleotides at 5'-ends of the integrated viral DNA and ligation of the single strand breaks within integration intermediate (Lesbats et al., 2016). The repair stage is crucial for the viral life cycle since integrated-unrepaired (I–U) proviral DNA will not lead to an effective production of viral proteins. Moreover, a failure of genomic gap repair might even result in apoptosis of the infected cell. A correct assessment of the amount of an I–U DNA directly after integration will help to study the cellular repair machinery involved in the lentiviral DNA integration and in the development of a novel type of HIV-1 inhibitors blocking post-integration gap repair stage.

A variety of knockdown and knockout studies showed the contribution of nearly all DNA repair pathways for HIV life cycle (Baekelandt et al., 2000; Daniel et al., 2001; Espeseth et al., 2011), but all of these works based their conclusions only on circumstantial evidence: production of viral (e.g. p24) or vector reporter genes (luciferase, GFP, etc.) (Brass et al., 2008; Espeseth et al., 2011; Zhou et al., 2008), relative level of integrated DNA and circular 1-LTR and 2-LTR viral DNA forms, that result from an unsuccessful completion of integration (Li et al., 2001), mutations around integration sites (Sakurai et al., 2009; Taganov et al., 2001), post-transduction cell survival and proliferation (Daniel et al., 2004). These approaches do not enable direct and precise measurement of the amount of integrated-repaired (I–R) proviral DNA. The previously published qPCR-based assays for a precise measurement of various viral DNA forms could not discriminate between I–R and I–U forms. As a result, integrated-unrepaired DNA that would not provide an effective production of viral proteins is included in the data.

Using a previously published qPCR technique for the measurement of reverse-transcribed, circular and integrated DNA forms (Vandergeeten et al., 2014), we have developed a modified protocol that incorporates a single preamplification step for an assessment of fully repaired provirus, termed here as I–R form. Separately, the total integrated DNA is measured following an original protocol (Vandergeeten et al., 2014). Thus, a fraction of I–R proviral DNA among the whole bulk of integrated viral DNA can be assessed.

We used this modified protocol to study the kinetics of post-integrational gap repair on a VSV-G pseudotyped HIV-1 derived vector (Mazurov et al., 2010). The use of replication-incompetent vector allowed us to precisely measure the kinetics of gap repair as there is no reinfection by newly formed viral particles. While an integrated proviral DNA can be detected as early as 8–9 h.p.i., the amount of I–R DNA only started to increase after 17 h.p.i. This is a direct indication that at

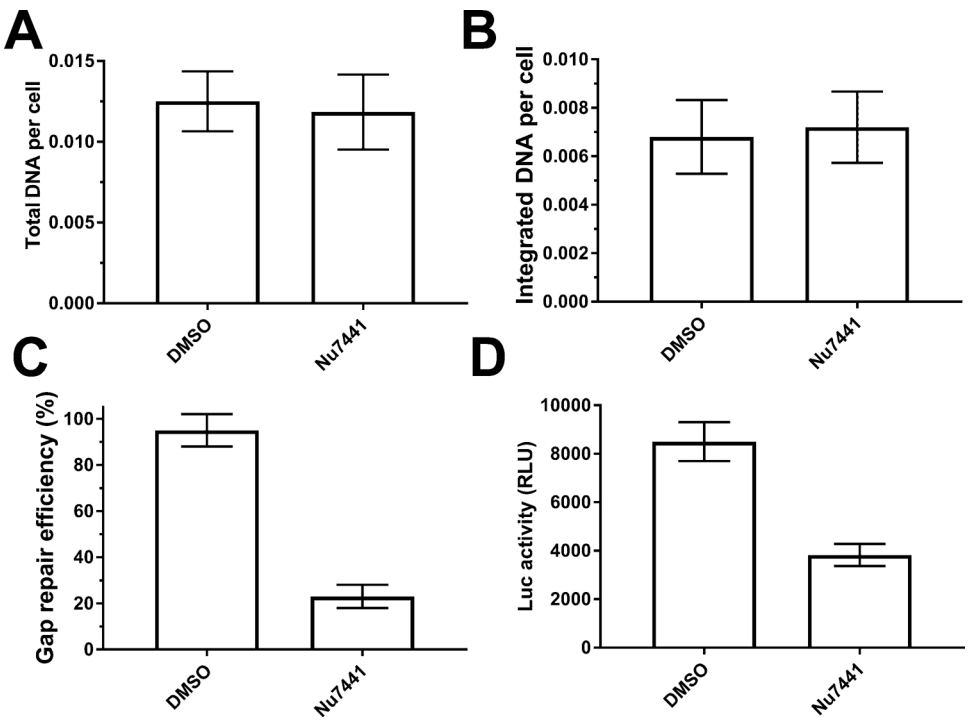

Fig. 4. Effect of DNA-PKcs inhibition by Nu7441 on post-integrational gap repair efficiency in HEK 293T cells treated by DMSO (control) or Nu7441 and transduced by VSV-G pseudotyped single round HIV-based vector (27 h.p.i.). The level of total viral DNA (A), integrated DNA (B), efficiency of gap repair (C) and relative luciferase level (D).

least in our model proviral system the gap repair process lasts for about 8–9 h post integration (Fig. 3E).

We also performed experiments to validate our assay on a system where the function of a known DNA breaks repair factor could be inhibited. We chose to use the DNA-dependent protein kinase for this purpose as its positive role in the post-integration gap repair has been widely reported (Daniel et al., 2001, 1999; Skalka and Katz, 2005; Taganov et al., 2001). We used the Nu7441 compound to selectively inhibit the activity of the catalytic subunit of DNA-PK. The cell treatment by Nu7441 leads to a significant drop in the expression of vector reporter protein (Fig. 4D). Using the gap repair estimation method presented here, we have directly shown for the first time that the inhibition of the DNA-PKcs and a concomitant block in the NHEJ DNA repair pathway leads to a ~4.3 fold drop in the post-integrational gap repair efficiency (Fig. 4C). Importantly, the decrease in the luciferase level correlates with the decrease in the post-integrational repair level, and this fact indicates once again that I–U proviral DNA cannot serve as a template for the synthesis of viral proteins. Of note, no decrease in the amount of total or integrated DNA can be observed under conditions used in our work (Fig. 4A–B). Altogether these data provide direct evidence for a significant role of DNA-PK and the NHEJ repair pathway in the post-integration repair of the HIV-1 integration intermediate. Thus, the assay presented here provides a useful tool for studying the role of different factors in the post-integration gap repair of HIV-1 as well as of other members of the Retroviridae family. It can be further used to study the role of other DNA repair pathways within the post-integrational gap repair in experimental systems that are close to *in vivo* conditions. Furthermore, the method can be adapted to study the post-integrational repair with other retroviruses, endogenous retroviruses and other viruses from different genera that may have similar integration process.

Author contributions

The experiments were conceived and designed by ANA, ESK, MBG. The experiments were performed by ANA, ESK. The data were analyzed by ANA, ESK, MBG. ANA, ESK, MGI, MBG contributed to the writing and revision of the manuscript. ANA, ESK, MGI, MBG agree with the manuscript's results and conclusions.

Acknowledgements

This work was supported by the Russian Science Foundation grant 17-14-01107. The authors thank Dr. D.V. Mazurov for his kind gift of pUCHR_inLuc HIV genomic plasmid.

Appendix A. Supplementary data

Supplementary material related to this article can be found, in the online version, at doi:https://doi.org/10.1016/j.jviromet.2018.09.004.

References

Ariumi, Y., Turelli, P., Masutani, M., Trono, D., 2005. DNA damage sensors ATM, ATR, DNA-PKcs, and PARP-1 are dispensable for human immunodeficiency virus type 1 integration DNA damage sensors ATM, ATR, DNA-PKcs, and PARP-1 are dispensable for human immunodeficiency virus type 1 integration. Society 79, 2973–2978. https://doi.org/10.1128/JVI.79.5.2973.

Baekelandt, V., Claeys, A., Cherepanov, P., De Clercq, E., De Strooper, B., Nuttin, B., Debyser, Z., 2000. DNA-dependent protein kinase is not required for efficient lentivirus integration. J. Virol. 74, 11278–11285. https://doi.org/10.1128/JVI.74.23.11278-11285.2000.

Bennett, G.R., Peters, R., Wang, X.H., Hanne, J., Sobol, R.W., Bundschuh, R., Fishel, R., Yoder, K.E., 2014. Repair of oxidative DNA base damage in the host genome influences the HIV integration site sequence preference. PLoS One 9, 3–9. https://doi.org/10.1371/journal.pone.0103164.

Brass, A.L., Dykxhoorn, D.M., Benita, Y., Yan, N., Engelman, A., Xavier, R.J., Lieberman, J., Elledge, S.J., Xavier, R., 2008. Identification of host proteins required for HIV infection through a functional genomic screen. Science 319, 921–926. https://doi.org/10.1126/science.1152725.

Cimarelli, A., Darlix, J.L., 2014. HIV-1 reverse transcription. Methods Mol. Biol. 1087, 55–70. https://doi.org/10.1007/978-1-62703-670-2_6.

Cooper, A., García, M., Petrovas, C., Yamamoto, T., Koup, Ra, Nabel, G.J., 2013. HIV-1 causes CD4 cell death through DNA-dependent protein kinase during viral integration. Nature 498, 376–379. https://doi.org/10.1038/nature12274.

Daniel, R., Katz, R.A., Skalka, A.M., 1999. A role for DNA-PK in retroviral DNA integration. Science 284, 644–647. https://doi.org/10.1126/science.284.5414.644.

Daniel, R., Katz, R.A., Merkel, G., Hittle, J.C., Yen, T.J., Skalka, A.M., 2001. Wortmannin potentiates integrase-mediated killing of lymphocytes and reduces the efficiency of stable transduction by retroviruses. Mol. Cell. Biol. 21, 1164–1172. https://doi.org/10.1128/MCB.21.4.1164-1172.2001.

Daniel, R., Greger, J.G., Katz, Ra, Taganov, K.D., Wu, X., Kappes, J.C., Skalka, A.M., 2004. Evidence that stable retroviral transduction and cell survival following DNA

integration depend on components of the nonhomologous end joining repair pathway. J. Virol. 78, 8573–8581. https://doi.org/10.1128/JVI.78.16.8573-8581.2004.
Delelis, O., Carayon, K., Saïb, A., Deprez, E., Mouscadet, J.F., 2008. Integrase and integration: biochemical activities of HIV-1 integrase. Retrovirology 5, 114. https://doi.org/10.1186/1742-4690-5-114.
Engelman, A., Mizuuchi, K., Craigie, R., 1991. HIV-1 DNA integration: mechanism of viral DNA cleavage and DNA strand transfer. Cell 67, 1211–1221. https://doi.org/10.1016/0092-8674(91)90297-C.
Espeseth, A.S., Fishel, R., Hazuda, D., Huang, Q., Xu, M., Yoder, K., Zhou, H., 2011. Sirna screening of a targeted library of DNA repair factors in HIV infection reveals a role for base excision repair in HIV integration. PLoS One 6. https://doi.org/10.1371/journal.pone.0017612.
Fernandez, G., Zeichner, S.L., 2010. Cell line-dependent variability in HIV activation employing DNMT inhibitors. Virol. J. 7 (266). https://doi.org/10.1186/1743-422X-7-266.
Freed, E.O., Mouland, A.J., 2006. The cell biology of HIV-1 and other retroviruses. Retrovirology 3 (77). https://doi.org/10.1186/1742-4690-3-77.
Jeanson, L., Subra, F., Vaganay, S., Hervy, M., Marangoni, E., Bourhis, J., Mouscadet, J.-F., 2002. Effect of Ku80 depletion on the preintegrative steps of HIV-1 replication in human cells. Virology 300, 100–108. https://doi.org/10.1006/viro.2002.1515.
Knyazhanskaya, E.S., Shadrina, O.A., Anisenko, A.N., Gottikh, M.B., 2016. Role of DNA-dependent protein kinase in the HIV-1 replication cycle. Mol. Biol. Orig. Russ. Text© 50, 26–8933. https://doi.org/10.1134/S0026893316040075.
König, R., Zhou, Y., Elleder, D., Diamond, T.L., Bonamy, G.M.C., Irelan, J.T., Chiang, C., yuan, Tu, B.P., De Jesus, P.D., Lilley, C.E., Seidel, S., Opaluch, A.M., Caldwell, J.S., Weitzman, M.D., Kuhen, K.L., Bandyopadhyay, S., Ideker, T., Orth, A.P., Miraglia, L.J., Bushman, F.D., Young, J.A., Chanda, S.K., 2008. Global analysis of host-pathogen interactions that regulate early-stage HIV-1 replication. Cell 135, 49–60. https://doi.org/10.1016/j.cell.2008.07.032.
Leahy, J.J.J., Golding, B.T., Griffin, R.J., Hardcastle, I.R., Richardson, C., Rigoreau, L., Smith, G.C.M., 2004. Identification of a highly potent and selective DNA-dependent protein kinase (DNA-PK) inhibitor (NU7441) by screening of chromenone libraries. Bioorg. Med. Chem. Lett. 14, 6083–6087. https://doi.org/10.1016/j.bmcl.2004.09.060.
Lesbats, P., Engelman, A.N., Cherepanov, P., 2016. Retroviral DNA integration. Chem. Rev. 116, 12730–12757. https://doi.org/10.1021/acs.chemrev.6b00125.
Lewinski, M.K., Bushman, F.D., 2005. Retroviral DNA integration–mechanism and consequences. Adv Genet. 55, 147–181. https://doi.org/10.1016/S0065-2660(05)55005-3.
Li, L., Olvera, J.M., Yoder, K.E., Mitchell, R.S., Butler, S.L., Lieber, M., Martin, S.L., Bushman, F.D., 2001. Role of the non-homologous DNA end joining pathway in the early steps of retroviral infection. EMBO J. 20, 3272–3281. https://doi.org/10.1093/emboj/20.12.3272.
Ma, Y., Schwarz, K., Lieber, M.R., 2005. The artemis: DNA-PKcs endonuclease cleaves DNA loops, flaps, and gaps. DNA Repair. (Amst) 4, 845–851. https://doi.org/10.1016/j.dnarep.2005.04.013.
Mazurov, D., Ilinskaya, A., Heidecker, G., Lloyd, P., Derse, D., 2010. Quantitative comparison of HTLV-1 and HIV-1 cell-to-cell infection with new replication dependent vectors. PLoS Pathog. 6. https://doi.org/10.1371/journal.ppat.1000788.
Sakurai, Y., Komatsu, K., Agematsu, K., Matsuoka, M., 2009. DNA double strand break repair enzymes function at multiple steps in retroviral infection. Retrovirology 6 (114). https://doi.org/10.1186/1742-4690-6-114.
Skalka, A.M., Katz, R.A., 2005. Retroviral DNA integration and the DNA damage response. Cell Death Differ. 12, 971–978. https://doi.org/10.1038/sj.cdd.4401573.
Smith, J.A., Wang, F.-X., Zhang, H., Wu, K.-J., Williams, K.J., Daniel, R., 2008. Evidence that the Nijmegen breakage syndrome protein, an early sensor of double-strand DNA breaks (DSB), is involved in HIV-1 post-integration repair by recruiting the ataxia telangiectasia-mutated kinase in a process similar to, but distinct from, cellular DSB repair. Virol. J. 5, 11. https://doi.org/10.1186/1743-422X-5-11.
Taganov, K., Daniel, R., Katz, Ra, Favorova, O., Skalka, a M., 2001. Characterization of retrovirus-host DNA junctions in cells deficient in nonhomologous-end joining. J. Virol. 75, 9549–9552. https://doi.org/10.1128/JVI.75.19.9549-9552.2001.
Vandergeeten, C., Fromentin, R., Merlini, E., Lawani, M.B., DaFonseca, S., Bakeman, W., McNulty, A., Ramgopal, M., Michael, N., Kim, J.H., Ananworanich, J., Chomont, N., 2014. Cross-clade ultrasensitive PCR-based assays to measure HIV persistence in large-cohort studies. J. Virol. 88, 12385–12396. https://doi.org/10.1128/JVI.00609-14.
Yoder, K.E., Bushman, F.D., 2000. Repair of gaps in retroviral DNA integration intermediates. J. Virol. 74, 11191–11200. https://doi.org/10.1128/JVI.74.23.11191-11200.2000.
Yoder, K.E., Espeseth, A., Wang, X., Fang, Q., Russo, M.T., Lloyd, R.S., Hazuda, D., Sobol, R.W., Fishel, R., 2011. The base excision repair pathway is required for efficient lentivirus integration. PLoS One 6, e17862. https://doi.org/10.1371/journal.pone.0017862.
Zhou, H., Xu, M., Huang, Q., Gates, A.T., Zhang, X.D., Castle, J.C., Stec, E., Ferrer, M., Strulovici, B., Hazuda, D.J., Espeseth, A.S., 2008. Genome-scale RNAi screen for host factors required for HIV replication. Cell Host Microbe 4, 495–504. https://doi.org/10.1016/j.chom.2008.10.004.